AIMS Mathematics, 11(8): 23847–23867.
DOI: 10.3934/math.2026960
Received: 02 May 2026
Revised: 27 June 2026
Accepted: 08 July 2026
Published: 04 August 2026

https://www.aimspress.com/journal/Math

Research article

Analysis of a delayed EBV oncovirus dynamics model

Azizah Alrajhi[1] **and Afnan D. Al Agha**[2,*]

[1] Department of Mathematics, Faculty of Science, King Abdulaziz University, P.O. Box 80203, Jeddah 21589, Saudi Arabia

[2] Department of Mathematical Science, College of Engineering, University of Business and Technology, Jeddah 21361, Saudi Arabia

* **Correspondence:** Email: a.alagha@ubt.edu.sa.

Abstract: About 1.5% of all cancers worldwide are attributed to the Epstein-Barr Virus (EBV). Mathematical models have been used to support clinical trials in identifying potential treatments for many diseases. This paper proposes a delayed within-host model of EBV oncovirus dynamics. The model analyzes the interactions between uninfected B cells, actively infected B cells, latently infected B cells, cancerous infected B cells, EBV particles, and cytotoxic T lymphocytes (CTLs). We establish the nonnegativity and boundedness of the model solutions. We derive all equilibrium points and demonstrate their local stability. We execute sensitivity analyses of the reproduction numbers $\mathcal{R}_V$ and $\mathcal{R}_I$. We conduct several numerical simulations. Based on our results, increasing the value of a_1, which measures the role of the EBV in weakening the ability of CTLs to kill infected cells, raises the concentration of infected B cells in the body. This can lead to more severe EBV infections. Moreover, increasing the value of a_2, which measures the role of the EBV in impairing the natural death of cancer cells, increases the concentration of cancer cells in the body. In addition, increasing the values of the time delays in the absence of CTLs increases the concentration of healthy cells and reduces the concentrations of actively infected cells and cancer cells. Additionally, the results show that the basic reproduction number $\mathcal{R}_V$ is sensitive to the proliferation rate of the EBV, the production rate of uninfected cells, the infection rate, and the death rates of uninfected and actively infected cells. Thus, the values of these parameters should be carefully estimated.

Keywords: B cells; EBV; oncovirus; cancer; stability
Mathematics Subject Classification: 34K20, 37N25, 92B05, 92C50

1. Introduction

About 12% of viral infections can result in cancer [1,2]. These infections are caused by oncoviruses. Cancer development requires chronic inflammation, immunosuppression, or disruption of normal cell growth [1, 2]. Viral cancers usually need 15 to 40 years to develop [1]. An exception is EBV-associated lymphoproliferative disease which may occur shortly after infection [1]. Notably, viral replication in cancers is suppressed, as active replication can kill the host cell and prevent cancer development [1]. Some well-recognized oncoviruses are the Epstein-Barr Virus (EBV), Hepatitis B Virus (HBV), Hepatitis C Virus (HCV), Human Papillomavirus (HPV), and Human T-lymphotropic Virus (HTLV-1) [1–3].

The EBV is a DNA virus that belongs to the Herpesviridae family [1, 4]. The EBV was discovered in Burkitt's lymphoma cells in 1964 [1]. About 1.5% of all cancers worldwide are attributed to the EBV. The EBV primarily infects B lymphocytes via binding of the viral protein gp350 to the B cell receptor CD21 [1, 5]. After primary infection, the EBV enters a latent state, leading to latent infection in B cells [1, 4, 6]. During latency, the virus remains non-lytic and does not generate new virions [4, 7]. However, partial lytic activity has been suggested as a mechanism that allows persistent low-level replication without progression to a fully productive infection [8]. Many EBV genes are expressed during the latent phase, which may contribute to cancer development and immune escape [1, 4]. EBV persistence is partly attributed to its ability to evade host immune responses. In particular, latently infected cells and EBV-associated malignant cells express a restricted range of viral antigens and may impair antigen presentation, thereby reducing their recognition by cytotoxic T lymphocytes (CTLs) [1, 2, 4, 6, 7]. In contrast, actively infected cells express higher levels of viral antigens and are therefore more susceptible to CTL-mediated killing [1, 2, 4, 6, 7]. The EBV-associated lymphoproliferative disorders include Burkitt's lymphoma, Hodgkin's lymphoma, and post-transplant lymphoproliferative disease [1, 2, 9]. The strong link between the EBV and many cancers highlights the need to understand EBV infection to develop effective treatments [1, 2].

Mathematical modeling has been used to support clinical trials in identifying potential treatments for many infections and diseases. Numerous models have been developed to study infections such as the Human Immunodeficiency Virus (HIV) [10–13], HBV [14–16], HCV [17–19], measles [20], malaria [21], chlamydia [22], and COVID-19 [23–27]. Many other infections have also been studied [28–30]. In addition, a substantial number of models have been generated to understand the relationship between some viruses and cancer. These models can be divided into oncolytic virus models [31–33], and oncovirus models [3]. However, based on our current knowledge, studies related to oncovirus models are rare. In [3], a mathematical model was used to explore how the viral life cycle could affect oncogenesis at the within-host and between-host levels. The model was analyzed from a biological perspective, and no mathematical analysis was performed. To the best of our knowledge, no within-host models of EBV infection have been previously studied from a mathematical perspective.

In this work, we formulate a within-host EBV oncovirus dynamics model composed of six delay differential equations (DDEs) that analyze the interactions between uninfected B cells, actively infected B cells, latently infected B cells, cancerous infected B cells, EBV particles, and CTLs. EBV infection involves several biological processes that are not instantaneous and are characterized by intrinsic time lags, including viral replication, the establishment of latency, and the progression from latent infection to malignancy. Therefore, DDEs offer a more realistic framework than ordinary differential equations

(ODEs) by explicitly accounting for the time required for these biological processes to occur. We establish the nonnegativity and boundedness of the model solutions. We derive all equilibrium points and demonstrate their local stability. We execute sensitivity analyses of the threshold numbers $\mathcal{R}_V$ and $\mathcal{R}_I$. Moreover, we conduct numerical simulations and discuss the results.

2. Oncogenic EBV model

The model is formulated based on the following assumptions:

(i) B cells are generated from a source at a constant rate, while they are depleted due to EBV infection and natural death;

(ii) The depletion of actively infected B cells occurs as a result of CTL clearance and natural death;

(iii) A proportion of actively infected B cells turns into latently infected B cells;

(iv) A proportion of latently infected B cells turns into cancer cells;

(v) The multistage carcinogenic process is represented by a single effective transition rate, ρ_3, which reflects the average progression from latent infection to the cancerous state;

(vi) Both latent and cancer cells die at natural rates;

(vii) Some delays occur during the transitions to active infection, latency, and the cancerous state;

(viii) EBV particles are only produced by actively infected cells, while they decay at a constant rate;

(ix) CTLs are stimulated by actively infected cells, while their depletion occurs due to natural death.

The model is structured as follows:

$$\begin{cases} \dot{F}(t) = \theta - \rho_1 F(t)V(t) - \epsilon_1 F(t), \\ \dot{A}(t) = \rho_1 e^{-r_1\tau_1} F(t-\tau_1)V(t-\tau_1) - (1-a_1)\gamma A(t)I(t) - (\rho_2+\epsilon_2)A(t), \\ \dot{L}(t) = \rho_2 e^{-r_2\tau_2} A(t-\tau_2) - (\rho_3+\epsilon_3)L(t), \\ \dot{C}(t) = \rho_3 e^{-r_3\tau_3} L(t-\tau_3) - (1-a_2)\epsilon_4 C(t), \\ \dot{V}(t) = \eta A(t) - \epsilon_5 V(t), \\ \dot{I}(t) = \alpha A(t)I(t) - \epsilon_6 I(t), \end{cases} \tag{2.1}$$

where $(F, A, L, C, V, I)(t)$ measure the concentrations of uninfected B cells, actively infected B cells, latently infected B cells, cancerous infected B cells, EBV particles, and CTLs at time t, respectively. Uninfected cells are generated at a steady rate θ, become infected by the EBV at a rate $\rho_1 FV$, and die at a rate $\epsilon_1 F$. Actively infected cells proliferate at a rate $\rho_1 e^{-r_1\tau_1} F(t-\tau_1)V(t-\tau_1)$, and turn into latent cells at a rate $\rho_2 A$. Latent cells turn into cancerous cells at a rate $\rho_3 L$. Actively infected cells, latent cells, and cancerous cells die naturally at rates $\epsilon_2 A$, $\epsilon_3 L$, and $(1-a_2)\epsilon_4 C$, respectively. EBV particles are produced by actively infected cells at a rate ηA, while they decay at a rate $\epsilon_5 V$. CTLs are induced by active cells at a rate αAI, while they die at a rate $\epsilon_6 I$. The parameter a_1 measures the effect of the oncogenic virus in reducing CTL-mediated killing of infected cells, where $a_1 \in [0, 1)$. In addition, the parameter a_2 measures the impact of the oncogenic virus in reducing the death of

cancerous cells, where $a_2 \in [0, 1)$. The delay $\tau_1 > 0$ represents the period from virus entry into B cells until their conversion into actively infected cells. The delay $\tau_2 > 0$ is the time needed by actively infected cells to enter the latent mode. The delay $\tau_3 > 0$ is the time needed by latent cells to convert into cancer cells. In addition, $e^{-r_i\tau_i}(i = 1, 2, 3)$ represent the survival probabilities from $t - \tau_i$ to t, where r_i represent the death rates during the delay periods. The parameters r_i capture not only natural cell death but also other biological factors that may prevent successful progression, such as immune-mediated clearance, unsuccessful establishment of infection or latency, and cellular dysfunction during the transition process.

3. Properties of the solutions

This section discusses the well-posedness of the solutions and computes all possible equilibrium points of model (2.1).

3.1. Nonnegativity and boundedness

Let $\mathcal{X} = C([-\tau^b, 0], \mathbb{R}^6_+)$, where $\tau^b = \max\{\tau_1, \tau_2, \tau_3\}$, be the Banach space of continuous functions with norm $\|\psi_i\| = \sup_{-\tau^b \le \omega \le 0} |\psi_i(\omega)|$ for $\psi_i \in C([-\tau^b, 0], \mathbb{R}^6_+)$, $i = 1, 2, ..., 6$.

The initial conditions for model (2.1) are

$$\begin{cases} (F, A, L, C, V, I)(\omega) = (\psi_1, \psi_2, \psi_3, \psi_4, \psi_5, \psi_6)(\omega), \\ \psi_i(\omega) \ge 0, i = 1, 2, ..., 6, \quad \omega \in [-\tau^b, 0]. \end{cases} \tag{3.1}$$

The standard theory of functional differential equations guarantees that model (2.1) with initial conditions (3.1) has a unique solution [34, 35].

Theorem 3.1. *All solutions of model* (2.1) *with conditions* (3.1) *are nonnegative and ultimately bounded.*

Proof. From the first equation of model (2.1), it follows that

$$\dot{F}|_{F=0} = \theta > 0, \quad \dot{I}|_{I=0} = 0.$$

Thus, $F(t), I(t) \ge 0 \ \forall \ t \ge 0$. Additionally, for $t \in [0, \tau^b]$, we have the following:

$$\begin{aligned}
A(t) &= \psi_2(0)e^{-\int_0^t [(1-a_1)\gamma I(u)+(\rho_2+\epsilon_2)]du} + \rho_1 e^{-r_1\tau_1} \int_0^t e^{-\int_s^t [(1-a_1)\gamma I(u)+(\rho_2+\epsilon_2)]du} F(s-\tau_1)V(s-\tau_1)ds, \\
L(t) &= \psi_3(0)e^{-(\rho_3+\epsilon_3)t} + \rho_2 e^{-r_2\tau_2} \int_0^t e^{-(\rho_3+\epsilon_3)(t-s)} A(s-\tau_2)ds, \\
C(t) &= \psi_4(0)e^{-(1-a_2)\epsilon_4 t} + \rho_3 e^{-r_3\tau_3} \int_0^t e^{-(1-a_2)\epsilon_4(t-s)} L(s-\tau_3)ds, \\
V(t) &= \psi_5(0)e^{-\epsilon_5 t} + \eta \int_0^t e^{-\epsilon_5(t-s)} A(s)ds.
\end{aligned}$$

This implies that $(A, L, C, V)(t) \ge 0 \ \forall \ t \in [0, \tau^b]$. By induction, we obtain $(A, L, C, V)(t) \ge 0 \ \forall \ t \ge 0$. This proves that all solutions are nonnegative.

Next, we show the boundedness of the solutions. From the first equation of model (2.1), we have

$$\dot{F}(t) \leq \theta - \epsilon_1 F(t) \implies \limsup_{t\to\infty} F(t) \leq \frac{\theta}{\epsilon_1}.$$

Let us introduce the following:

$$\mathcal{B}(t) = e^{-r_1\tau_1}F(t-\tau_1) + A(t) + \frac{(1-a_1)\gamma}{\alpha}I(t).$$

Then, we obtain the following:

$$\begin{aligned}\dot{\mathcal{B}}(t) &= e^{-r_1\tau_1}\theta - e^{-r_1\tau_1}\epsilon_1 F(t-\tau_1) - (\rho_2+\epsilon_2)A(t) - \frac{(1-a_1)\gamma\epsilon_6}{\alpha}I(t)\\ &\leq \theta - \mu\left[e^{-r_1\tau_1}F(t-\tau_1) + A(t) + \frac{(1-a_1)\gamma}{\alpha}I(t)\right]\\ &= \theta - \mu\mathcal{B},\end{aligned}$$

where $\mu = \min\{\epsilon_1, \rho_2+\epsilon_2, \epsilon_6\}$. This gives the following:

$$\limsup_{t\to\infty} \mathcal{B}(t) \leq \frac{\theta}{\mu}.$$

Accordingly,

$$\limsup_{t\to\infty} A(t) \leq \frac{\theta}{\mu} \quad \text{and} \quad \limsup_{t\to\infty} I(t) \leq \frac{\alpha\theta}{(1-a_1)\gamma\mu}.$$

From the third equation of model (2.1), we obtain the following:

$$\dot{L}(t) \leq \frac{\rho_2\theta}{\mu} - (\rho_3+\epsilon_3)L(t) \implies \limsup_{t\to\infty} L(t) \leq \frac{\rho_2\theta}{\mu(\rho_3+\epsilon_3)}.$$

Similarly, we can conclude from the fourth and fifth equations of model (2.1) that

$$\limsup_{t\to\infty} C(t) \leq \frac{\rho_2\rho_3\theta}{(1-a_2)\mu(\rho_3+\epsilon_3)\epsilon_4} \quad \text{and} \quad \limsup_{t\to\infty} V(t) \leq \frac{\eta\theta}{\mu\epsilon_5}.$$

Thus, all solutions are bounded. □

3.2. Equilibrium points

Theorem 3.2. *There exist threshold numbers $\mathcal{R}_V > 0$ and $\mathcal{R}_I > 0$ such that model* (2.1) *has three equilibrium points:*

(i) The healthy equilibrium $\mathcal{Q}_0 = (F_0, 0, 0, 0, 0, 0)$ always exists;

(ii) The EBV immune-inactive equilibrium $\mathcal{Q}_1 = (F_1, A_1, L_1, C_1, V_1, 0)$ exists if $\mathcal{R}_V > 1$;

(iii) The EBV immune-active equilibrium $\mathcal{Q}_2 = (F_2, A_2, L_2, C_2, V_2, I_2)$ exists if $\mathcal{R}_I > 1$.

Proof. By solving the algebraic system

$$\begin{cases} 0 = \theta - \rho_1 FV - \epsilon_1 F, \\ 0 = \rho_1 e^{-r_1\tau_1} FV - (1-a_1)\gamma AI - (\rho_2+\epsilon_2)A, \\ 0 = \rho_2 e^{-r_2\tau_2} A - (\rho_3+\epsilon_3)L, \\ 0 = \rho_3 e^{-r_3\tau_3} L - (1-a_2)\epsilon_4 C, \\ 0 = \eta A - \epsilon_5 V, \\ 0 = \alpha AI - \epsilon_6 I, \end{cases}$$

we find that system (2.1) admits three equilibria:

(i) The healthy equilibrium $Q_0 = (F_0, 0, 0, 0, 0, 0) = (\frac{\theta}{\epsilon_1}, 0, 0, 0, 0, 0)$. Hence, Q_0 is always defined.

(ii) The EBV immune-inactive equilibrium $Q_1 = (F_1, A_1, L_1, C_1, V_1, 0)$. Its components are given by

$$F_1 = \frac{e^{r_1\tau_1}(\rho_2+\epsilon_2)\epsilon_5}{\eta\rho_1}, \quad A_1 = \frac{\epsilon_1\epsilon_5(\mathcal{R}_V-1)}{\eta\rho_1}, \quad L_1 = \frac{e^{-r_2\tau_2}\rho_2\epsilon_1\epsilon_5(\mathcal{R}_V-1)}{\eta\rho_1(\rho_3+\epsilon_3)},$$
$$C_1 = \frac{e^{-r_2\tau_2-r_3\tau_3}\rho_2\rho_3\epsilon_1\epsilon_5(\mathcal{R}_V-1)}{(1-a_2)\eta\rho_1\epsilon_4(\rho_3+\epsilon_3)}, \quad V_1 = \frac{\epsilon_1(\mathcal{R}_V-1)}{\rho_1},$$

where $\mathcal{R}_V = \dfrac{e^{-r_1\tau_1}\eta\theta\rho_1}{\epsilon_1\epsilon_5(\rho_2+\epsilon_2)}$. Consequently, Q_1 is defined when the basic reproduction number $\mathcal{R}_V > 1$. Biologically, $\mathcal{R}_V$ is the average number of newly infected cells that arise from one infected cell in the absence of the CTL immune response. Hence, it determines whether an EBV infection can be established and persist within the host.

(iii) The EBV immune-active equilibrium $Q_2 = (F_2, A_2, L_2, C_2, V_2, I_2)$. Its components are given by

$$F_2 = \frac{\alpha\theta\epsilon_5}{\alpha\epsilon_1\epsilon_5+\eta\rho_1\epsilon_6}, \quad A_2 = \frac{\epsilon_6}{\alpha}, \quad L_2 = \frac{e^{-r_2\tau_2}\rho_2\epsilon_6}{\alpha(\rho_3+\epsilon_3)}, \quad C_2 = \frac{e^{-r_2\tau_2-r_3\tau_3}\rho_2\rho_3\epsilon_6}{(1-a_2)\alpha\epsilon_4(\rho_3+\epsilon_3)},$$
$$V_2 = \frac{\eta\epsilon_6}{\alpha\epsilon_5}, \quad I_2 = \frac{(\rho_2+\epsilon_2)(\mathcal{R}_I-1)}{(1-a_1)\alpha},$$

where $\mathcal{R}_I = \dfrac{e^{-r_1\tau_1}\alpha\eta\theta\rho_1}{(\rho_2+\epsilon_2)(\alpha\epsilon_1\epsilon_5+\eta\rho_1\epsilon_6)}$. Thus, Q_2 exists when $\mathcal{R}_I > 1$. Specifically, $\mathcal{R}_I$ measures the ability of the EBV infection to stimulate and sustain the immune response.

□

4. Local stability of equilibria

By considering the linearized system of model (2.1), the characteristic equation at any equilibrium point $Q_i = (F_i, A_i, L_i, C_i, V_i, I_i)$ is given by the following:

$$\begin{vmatrix} -\rho_1 V_i - \epsilon_1 - y & 0 & 0 & 0 & -\rho_1 F_i & 0 \\ \rho_1 e^{-(y+r_1)\tau_1} V_i & -(1-a_1)\gamma I_i - (\rho_2+\epsilon_2) - y & 0 & 0 & \rho_1 e^{-(y+r_1)\tau_1} F_i & -(1-a_1)\gamma A_i \\ 0 & \rho_2 e^{-(y+r_2)\tau_2} & -(\rho_3+\epsilon_3) - y & 0 & 0 & 0 \\ 0 & 0 & \rho_3 e^{-(y+r_3)\tau_3} & -(1-a_2)\epsilon_4 - y & 0 & 0 \\ 0 & \eta & 0 & 0 & -\epsilon_5 - y & 0 \\ 0 & \alpha I_i & 0 & 0 & 0 & \alpha A_i - \epsilon_6 - y \end{vmatrix} = 0,$$

where y is an eigenvalue.

Theorem 4.1. *The healthy equilibrium $\mathcal{Q}_0$ of model* (2.1) *is locally asymptotically stable if $\mathcal{R}_V < 1$ and unstable if $\mathcal{R}_V > 1$.*

Proof. The characteristic equation at $\mathcal{Q}_0$ is given by the following:

$$(y+\epsilon_1)(y+\rho_3+\epsilon_3)\left[y+(1-a_2)\epsilon_4\right](y+\epsilon_6)\left[(y+\rho_2+\epsilon_2)(y+\epsilon_5)-e^{-(y+r_1)\tau_1}\eta\rho_1 F_0\right]=0. \tag{4.1}$$

For $\tau_1 = \tau_2 = \tau_3 = 0$, the characteristic equation at $\mathcal{Q}_0$ becomes the following:

$$(y+\epsilon_1)(y+\rho_3+\epsilon_3)\left[y+(1-a_2)\epsilon_4\right](y+\epsilon_6)\left(y^2+\phi_1 y+\phi_2\right)=0,$$

where

$$\begin{aligned}\phi_1 =&\rho_2+\epsilon_2+\epsilon_5,\\ \phi_2 =&(\rho_2+\epsilon_2)\epsilon_5-\eta\rho_1 F_0=(\rho_2+\epsilon_2)\epsilon_5(1-\mathcal{R}_V).\end{aligned}$$

Four of the eigenvalues are given by the following:

$$y_1=-\epsilon_1<0,\quad y_2=-(\rho_3+\epsilon_3)<0,\quad y_3=-(1-a_2)\epsilon_4<0,\quad y_4=-\epsilon_6<0. \tag{4.2}$$

Two of the eigenvalues are determined by the solution to the equation $y^2+\phi_1 y+\phi_2=0$, where $\phi_1>0$ and $\phi_2>0$ if $\mathcal{R}_V<1$. By the Routh-Hurwitz theorem, the roots of the equation are either negative or have negative real parts if $\mathcal{R}_V<1$. This implies that the eigenvalues of the characteristic equation at $\mathcal{Q}_0$ are either negative or have negative real parts if $\mathcal{R}_V<1$. On the other hand, at least one of the eigenvalues has a positive real part when $\mathcal{R}_V>1$. Therefore, $\mathcal{Q}_0$ is locally asymptotically stable if $\mathcal{R}_V<1$ and unstable if $\mathcal{R}_V>1$.

Next, we prove the stability for any $\tau_1>0$, $\tau_2>0$, and $\tau_3>0$. It is clear that Eq (4.1) has four negative eigenvalues, as shown in Eq (4.2). The remaining eigenvalues are determined by the following:

$$(y+\rho_2+\epsilon_2)(y+\epsilon_5)-e^{-(y+r_1)\tau_1}\eta\rho_1 F_0=0. \tag{4.3}$$

Equation (4.3) can be rewritten as follows:

$$(y+\rho_2+\epsilon_2)(y+\epsilon_5)=e^{-y\tau_1}(\rho_2+\epsilon_2)\epsilon_5\mathcal{R}_V. \tag{4.4}$$

If the real part of y is nonnegative, then the modulus of the left-hand side of (4.4) is as follows:

$$|(y+\rho_2+\epsilon_2)(y+\epsilon_5)|\geq(\rho_2+\epsilon_2)\epsilon_5. \tag{4.5}$$

The modulus of the right-hand side of (4.4) satisfies the following:

$$|e^{-y\tau_1}(\rho_2+\epsilon_2)\epsilon_5\mathcal{R}_V|\leq(\rho_2+\epsilon_2)\epsilon_5\mathcal{R}_V<(\rho_2+\epsilon_2)\epsilon_5. \tag{4.6}$$

Thus, Eqs (4.5) and (4.6) lead to a contradiction with Eq (4.4). This implies that all roots of Eq (4.1) have negative real parts, and $\mathcal{Q}_0$ is locally asymptotically stable if $\mathcal{R}_V<1$.

When $\mathcal{R}_V>1$, we introduce a function

$$f(y)=(y+\rho_2+\epsilon_2)(y+\epsilon_5)-e^{-(y+r_1)\tau_1}\eta\rho_1 F_0.$$

Note that $f(0)=(\rho_2+\epsilon_2)\epsilon_5(1-\mathcal{R}_V)<0$ and $\lim\limits_{y\to+\infty} f(y)=+\infty$. Hence, Eq (4.1) has at least one positive root. This shows that $\mathcal{Q}_0$ is unstable when $\mathcal{R}_V>1$. □

In the following theorems, we establish the local stability of Q_1 and Q_2 for zero time delays. The proofs of stability for positive time delays are left for future work. For $\tau_i > 0$, the characteristic equations for Q_1 and Q_2 become higher-order transcendental equations containing exponential terms $e^{-y\tau_i}$. This would require advanced analytical techniques, including imaginary-root analyses and the Hopf bifurcation theory, which are beyond the scope of the present study.

Theorem 4.2. *In the case of $\tau_1 = \tau_2 = \tau_3 = 0$, the EBV immune-inactive equilibrium Q_1 is locally asymptotically stable if $\mathcal{R}_V > 1$ and $\mathcal{R}_I < 1$. It is unstable when $\mathcal{R}_I > 1$.*

Proof. The characteristic equation at Q_1 is provided by the following:

$$(y + \rho_3 + \epsilon_3)\left[y + (1 - a_2)\epsilon_4\right](y - \alpha A_1 + \epsilon_6)\left(y^3 + \sigma_1 y^2 + \sigma_2 y + \sigma_3\right) = 0,$$

where

$$\begin{aligned}
\sigma_1 =& \epsilon_1 + \rho_1 V_1 + \rho_2 + \epsilon_2 + \epsilon_5 = \rho_2 + \epsilon_2 + \epsilon_5 + \epsilon_1 \mathcal{R}_V,\\
\sigma_2 =& (\rho_2 + \epsilon_2 + \epsilon_5)(\epsilon_1 + \rho_1 V_1) + (\rho_2 + \epsilon_2)\epsilon_5 - \eta\rho_1 F_1 = \epsilon_1(\rho_2 + \epsilon_2 + \epsilon_5)\mathcal{R}_V,\\
\sigma_3 =& (\epsilon_1 + \rho_1 V_1)(\rho_2 + \epsilon_2)\epsilon_5 - \eta\epsilon_1\rho_1 F_1 = \epsilon_1\epsilon_5(\rho_2 + \epsilon_2)(\mathcal{R}_V - 1).
\end{aligned}$$

Three of the eigenvalues are given by the following:

$$y_1 = -(\rho_3 + \epsilon_3) < 0, \quad y_2 = -(1 - a_2)\epsilon_4 < 0, \quad y_3 = \alpha A_1 - \epsilon_6 = \frac{\alpha\epsilon_1\epsilon_5 + \eta\rho_1\epsilon_6}{\eta\rho_1}(\mathcal{R}_I - 1) < 0 \quad \text{if} \quad \mathcal{R}_I < 1.$$

The remaining eigenvalues are determined by the solution to the equation $y^3 + \sigma_1 y^2 + \sigma_2 y + \sigma_3 = 0$. Note that $\sigma_1 > 0$, $\sigma_2 > 0$, and $\sigma_3 > 0$ if $\mathcal{R}_V > 1$. Additionally, we have the following:

$$\sigma_1\sigma_2 - \sigma_3 = \epsilon_1(\rho_2 + \epsilon_2)^2\mathcal{R}_V + (\epsilon_1\mathcal{R}_V + \epsilon_5)[\epsilon_1(\rho_2 + \epsilon_2 + \epsilon_5)\mathcal{R}_V] + \epsilon_1\epsilon_5(\rho_2 + \epsilon_2) > 0.$$

Thus, by the Routh-Hurwitz theorem, the roots of the equation $y^3 + \sigma_1 y^2 + \sigma_2 y + \sigma_3 = 0$ are either negative or have negative real parts if $\mathcal{R}_V > 1$. Accordingly, the eigenvalues of the characteristic equation at Q_1 are either negative or have negative real parts if $\mathcal{R}_V > 1$ and $\mathcal{R}_I < 1$. Furthermore, the eigenvalue $y_3 > 0$ if $\mathcal{R}_I > 1$. Therefore, Q_1 is locally asymptotically stable if $\mathcal{R}_V > 1$ and $\mathcal{R}_I < 1$, and unstable when $\mathcal{R}_I > 1$. □

Theorem 4.3. *In the case of $\tau_1 = \tau_2 = \tau_3 = 0$, the EBV immune-active equilibrium Q_2 is locally asymptotically stable if $\mathcal{R}_I > 1$.*

Proof. The characteristic equation at Q_2 can be written as follows:

$$(y + \rho_3 + \epsilon_3)\left[y + (1 - a_2)\epsilon_4\right]\left(y^4 + \delta_1 y^3 + \delta_2 y^2 + \delta_3 y + \delta_4\right) = 0,$$

where

$$\begin{aligned}
\delta_1 =& \gamma(1 - a_1)I_2 + \epsilon_1 + \rho_1 V_2 + \rho_2 + \epsilon_2 + \epsilon_5,\\
\delta_2 =& \alpha\gamma(1 - a_1)A_2 I_2 + (\epsilon_1 + \rho_1 V_2)[\gamma(1 - a_1)I_2 + \rho_2 + \epsilon_2 + \epsilon_5],\\
\delta_3 =& \alpha\gamma(1 - a_1)(\epsilon_1 + \rho_1 V_2 + \epsilon_5)A_2 I_2 + \rho_1 V_2\epsilon_5[\gamma(1 - a_1)I_2 + \rho_2 + \epsilon_2],\\
\delta_4 =& \alpha\gamma(1 - a_1)(\epsilon_1 + \rho_1 V_2)\epsilon_5 A_2 I_2.
\end{aligned}$$

Two of the eigenvalues are given by the following:

$$y_1 = -(\rho_3 + \epsilon_3) < 0, \quad y_2 = -(1 - a_2)\epsilon_4 < 0.$$

The other eigenvalues are determined by the solution to the equation $y^4 + \delta_1 y^3 + \delta_2 y^2 + \delta_3 y + \delta_4 = 0$. Since $A_2 > 0$ and $I_2 > 0$ when $\mathcal{R}_I > 1$, the coefficients δ_1, δ_2, δ_3 and δ_4 are positive when $\mathcal{R}_I > 1$. In addition, we have the following:

$$\begin{aligned}\delta_1\delta_2 - \delta_3 = \ & (\epsilon_1 + \rho_1 V_2)(\epsilon_1 + \rho_1 V_2 + \epsilon_5)[\gamma(1-a_1)I_2 + \rho_2 + \epsilon_2 + \epsilon_5] \\ & + [\gamma(1-a_1)I_2 + \rho_2 + \epsilon_2]\left[\alpha\gamma(1-a_1)A_2I_2 + (\epsilon_1 + \rho_1 V_2)(\gamma(1-a_1)I_2 + \rho_2 + \epsilon_2) + \epsilon_1\epsilon_5\right],\end{aligned}$$

$$\begin{aligned}& (\delta_1\delta_2 - \delta_3)\delta_3 - \delta_1^2\delta_4 \\ = \ & \alpha\gamma(1-a_1)A_2I_2[\gamma(1-a_1)I_2 + \rho_2 + \epsilon_2](\epsilon_1 + \rho_1 V_2) \\ & \times \left[(\epsilon_1 + \rho_1 V_2)^2 + \alpha\gamma(1-a_1)A_2I_2 + \epsilon_1\epsilon_5 + \epsilon_1 + \rho_1 V_2\right] \\ & + \rho_1 V_2\epsilon_5[\gamma(1-a_1)I_2 + \rho_2 + \epsilon_2][\alpha\gamma(1-a_1)A_2I_2\epsilon_5 + (\epsilon_1 + \rho_1 V_2)(\epsilon_1 + \rho_1 V_2 + \epsilon_5)(\gamma(1-a_1)I_2 \\ & + \rho_2 + \epsilon_2) + (\epsilon_1 + \rho_1 V_2)^2\epsilon_5 + \epsilon_1\epsilon_5^2] + \rho_1 V_2\epsilon_5[\gamma(1-a_1)I_2 + \rho_2 + \epsilon_2]^2 \\ & \times \left[\alpha\gamma(1-a_1)A_2I_2 + (\epsilon_1 + \rho_1 V_2)(\gamma(1-a_1)I_2 + \rho_2 + \epsilon_2) + \epsilon_1\epsilon_5\right] \\ & + \alpha\gamma(1-a_1)A_2I_2\rho_1 V_2\epsilon_5^2[\gamma(1-a_1)I_2 + \rho_2 + \epsilon_2]\left[-2 + \frac{\alpha\gamma(1-a_1)A_2I_2}{\rho_1 V_2\epsilon_5} + \frac{\rho_1 V_2\epsilon_5}{\alpha\gamma(1-a_1)A_2I_2}\right].\end{aligned}$$

From the relation between the arithmetic mean and geometric mean, we have the following:

$$-2 + \frac{\alpha\gamma(1-a_1)A_2I_2}{\rho_1 V_2\epsilon_5} + \frac{\rho_1 V_2\epsilon_5}{\alpha\gamma(1-a_1)A_2I_2} \geq 0.$$

Accordingly, $\delta_1\delta_2 - \delta_3 > 0$ and $(\delta_1\delta_2 - \delta_3)\delta_3 - \delta_1^2\delta_4 > 0$ when $\mathcal{R}_I > 1$. Hence, by the Routh-Hurwitz theorem, the eigenvalues of the characteristic equation at Q_2 are either negative or have negative real parts when $\mathcal{R}_I > 1$. This implies that the equilibrium Q_2 is locally asymptotically stable if $\mathcal{R}_I > 1$. □

5. Numerical simulations

In this section, numerical simulations are presented to confirm the results of Theorems 3.1, 3.2, 4.1–4.3. The MATLAB solver `dde23` is used to solve the equations of system (2.1) with three sets of initial conditions:

$$\begin{aligned}I-1 &: \Big(F(\omega), A(\omega), L(\omega), C(\omega), V(\omega), I(\omega)\Big) = (200, 0.01, 0.01, 0.01, 0.1, 5), \\ I-2 &: \Big(F(\omega), A(\omega), L(\omega), C(\omega), V(\omega), I(\omega)\Big) = (500, 0.001, 0.001, 0.02, 0.2, 10), \\ I-3 &: \Big(F(\omega), A(\omega), L(\omega), C(\omega), V(\omega), I(\omega)\Big) = (1000, 0.002, 0.003, 0.03, 0.3, 15),\end{aligned}$$

where $\omega \in [-\tau^b, 0]$. The values of α and ρ_1 are varied, while the remaining parameters take the values provided in Table 1. The following cases are obtained according to the stability of Q_0, Q_1, and Q_2:

(i) $\alpha = 10^{-7}$, $\rho_1 = 10^{-5}$, $\tau_1 = \tau_2 = \tau_3 = 0.1$: The solutions in this case (Figure 1) approach the equilibrium $Q_0 = (2000, 0, 0, 0, 0, 0)$, where $\mathcal{R}_V = 0.8617 < 1$. This result agrees with Theorem 4.1. It simulates the case of an individual without an EBV infection.

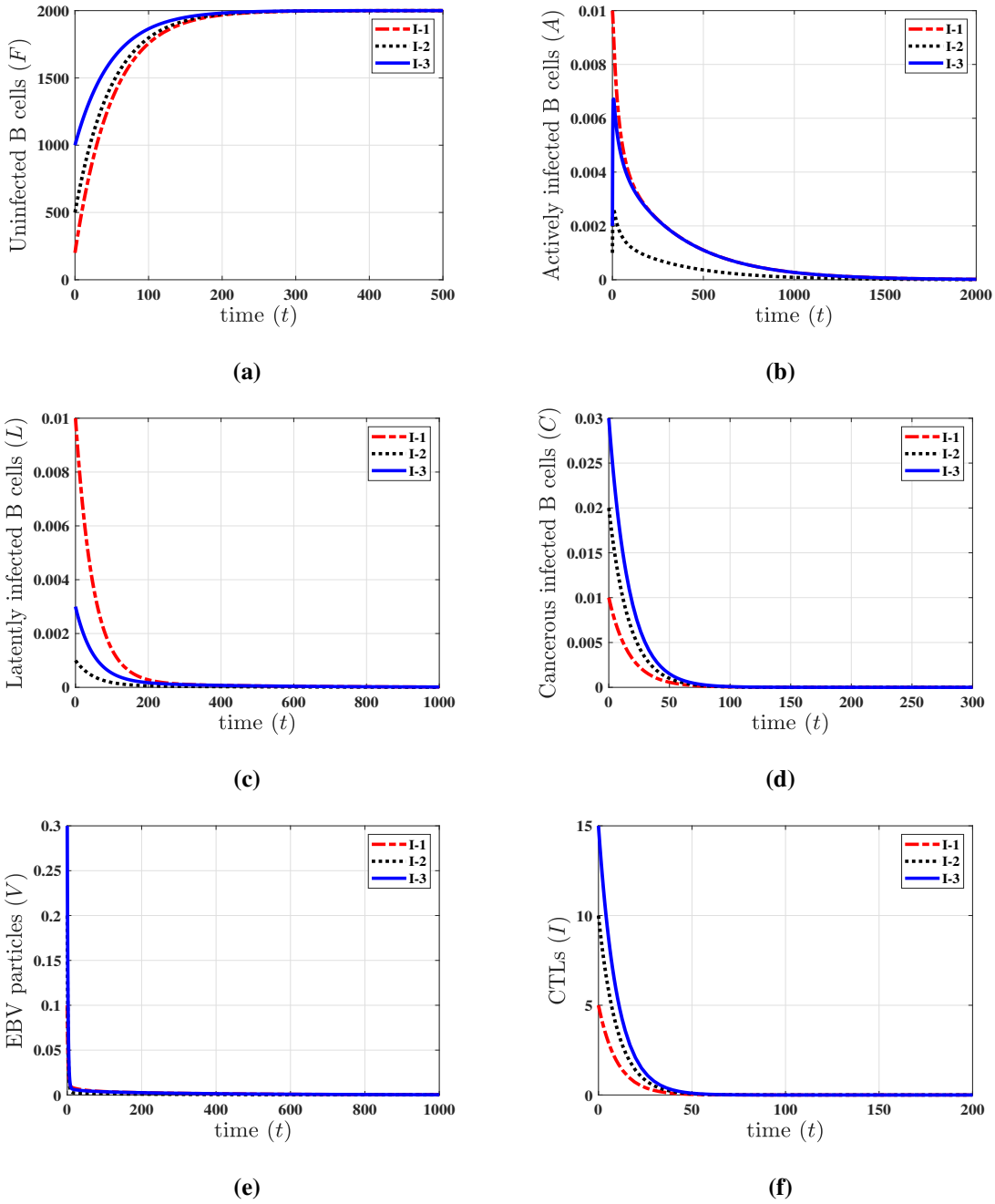

Figure 1. The numerical results of system (2.1) for $\alpha = 10^{-7}$ and $\rho_1 = 10^{-5}$ with three different sets of initial conditions: I-1=(200,0.01,0.01,0.01,0.1,5), I-2=(500,0.001,0.001,0.02,0.2,10), and I-3=(1000,0.002,0.003,0.03,0.3,15). The equilibrium $Q_0 = (2000, 0, 0, 0, 0, 0)$ is stable.

(ii) $\alpha = 10^{-7}$, $\rho_1 = 10^{-4}$, $\tau_1 = \tau_2 = \tau_3 = 0.1$: The solutions in this case (Figure 2) approach the point $Q_1 = (232, 1524, 65.64, 0.99, 1525, 0)$, where $\mathcal{R}_V = 8.6175 > 1$ and $\mathcal{R}_I = 0.0017 < 1$. This coincides closely with Theorem 4.2. Here, the person has a cancerous EBV infection with an inactive CTL immunity.

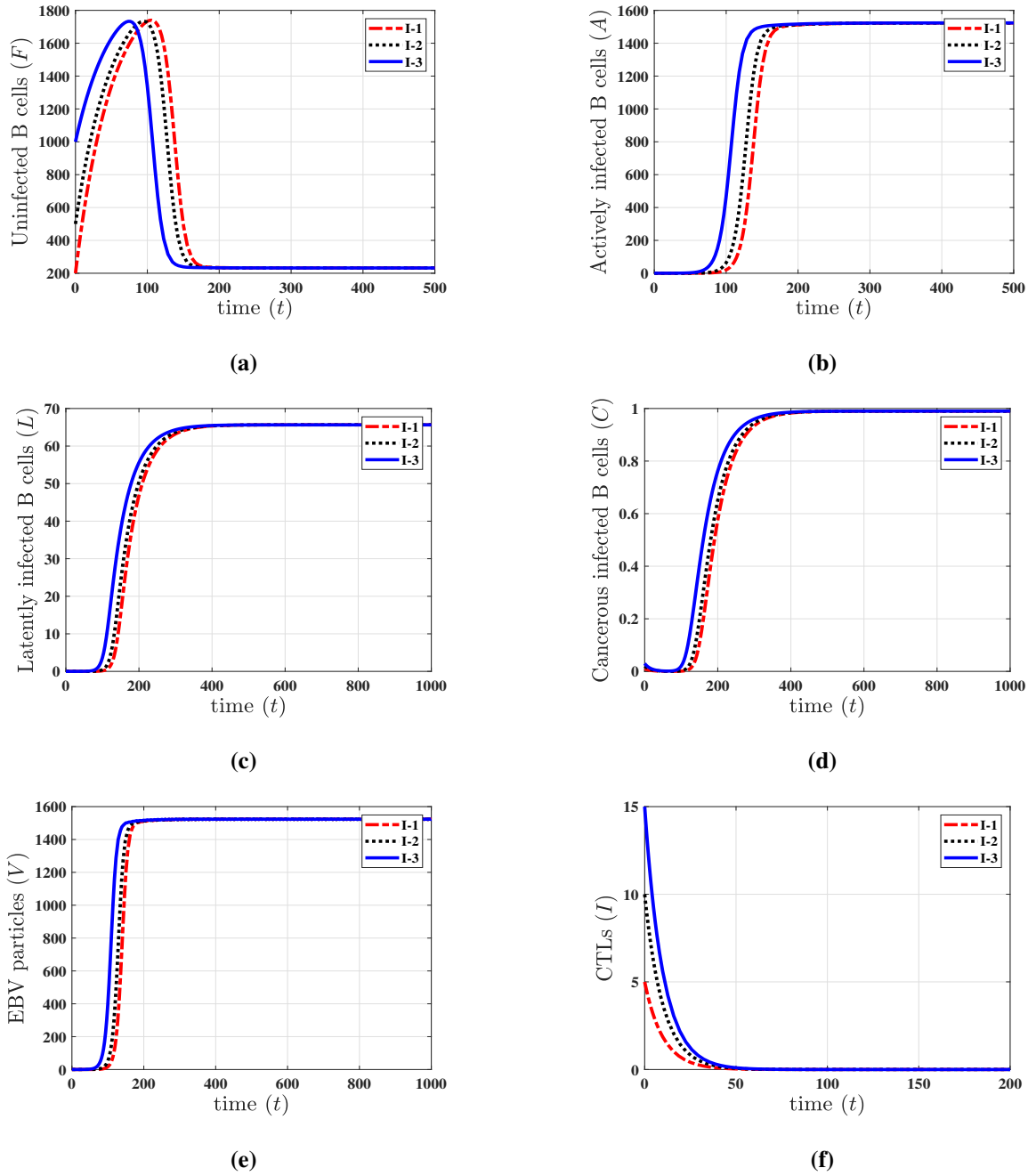

Figure 2. The numerical results of system (2.1) for $\alpha = 10^{-7}$ and $\rho_1 = 10^{-4}$ with three different sets of initial conditions: I-1=(200,0.01,0.01,0.01,0.1,5), I-2=(500,0.001,0.001,0.02,0.2,10), and I-3=(1000,0.002,0.003,0.03,0.3,15). The equilibrium $Q_1 = (232, 1524, 65.64, 0.99, 1525, 0)$ is stable.

(iii) $\alpha = 10^{-4}, \rho_1 = 10^{-3}, \tau_1 = \tau_2 = \tau_3 = 0.1$: The solutions (Figure 3) approach the equilibrium $Q_2 = (39.2, 1000, 43.09, 0.6498, 1000, 14.48)$, where $\mathcal{R}_I = 1.6897 > 1$. This agrees with Theorem 4.3. In this case, the CTL immunity is activated against the EBV infection.

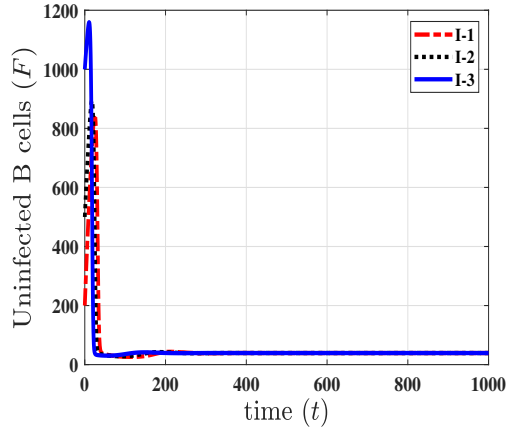

(a)

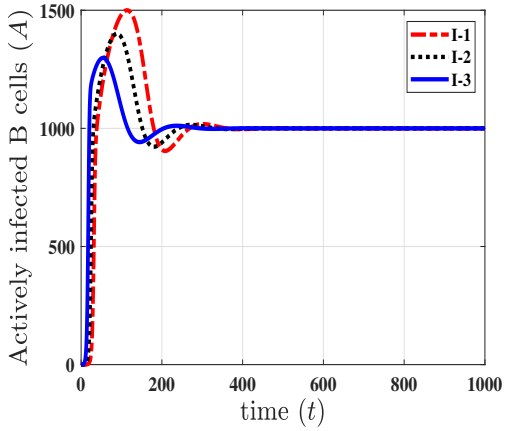

(b)

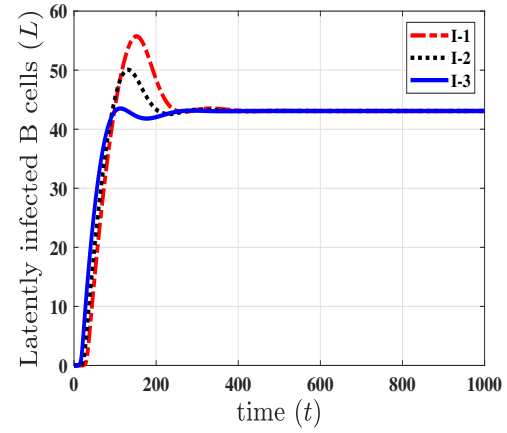

(c)

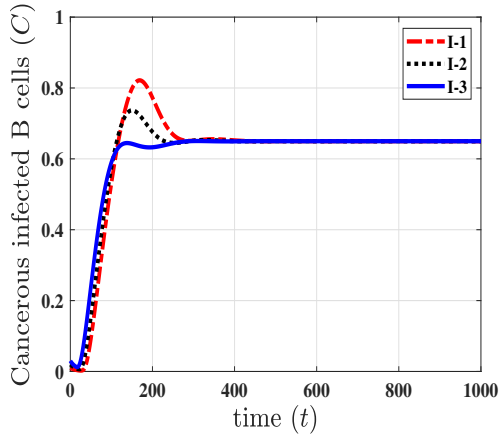

(d)

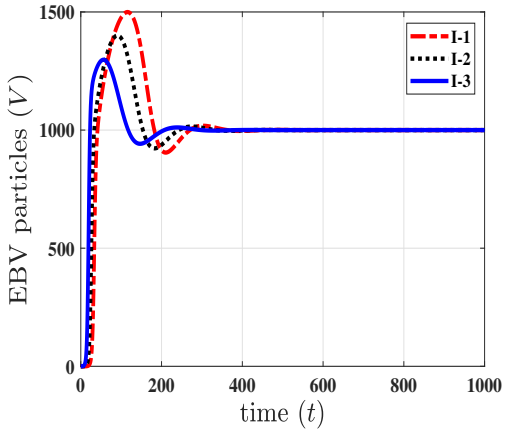

(e)

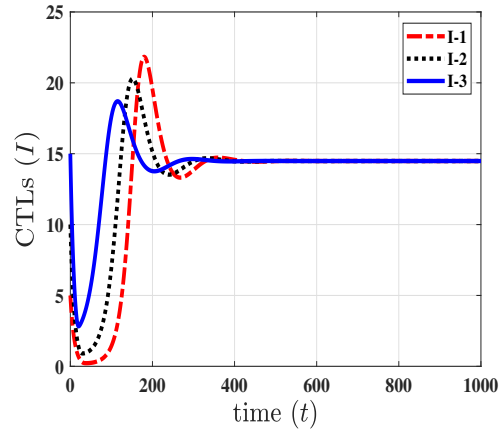

(f)

Figure 3. The numerical results of system (2.1) for $\alpha = 10^{-4}$ and $\rho_1 = 10^{-3}$ with three different sets of initial conditions: I-1=(200,0.01,0.01,0.01,0.1,5), I-2=(500,0.001,0.001,0.02,0.2,10), and I-3=(1000,0.002,0.003,0.03,0.3,15). The equilibrium $Q_2 = (39.2, 1000, 43.09, 0.6498, 1000, 14.48)$ is stable.

Table 1. Parameter values for system (2.1).

Parameter	Value	Source
θ	40	[36]
ρ_1	Varied	–
ρ_2	10^{-3}	Assumed
ρ_3	10^{-3}	Assumed
ϵ_1	0.02	[3]
ϵ_2	0.02	[3]
ϵ_3	0.02	[3]
ϵ_4	0.06	[32]
ϵ_5	0.5	[3]
ϵ_6	0.1	[24]
a_1	$0 \leq a_1 < 1$	–
a_2	$0 \leq a_2 < 1$	–
η	0.5	[3]
α	Varied	–
r_1	1	Assumed
r_2	1	Assumed
r_3	1	Assumed
τ_1	Varied	–
τ_2	Varied	–
τ_3	Varied	–
γ	10^{-3}	[3]

5.1. Effects of a_1 and a_2 on the model behavior

To investigate the impact of the oncogenic virus on CTLs, we consider case (iii) with different values of a_1. Figure 4(a) shows that increasing a_1 increases the concentration of CTLs in the body. As the virus inhibits CTLs from killing actively infected cells, this will raise the concentration of infected cells. As a result, the number of recruited CTLs will be higher.

On the other hand, to examine the effect of the oncogenic virus on cancer cells, we again consider case (iii) with different values of a_2. Figure 4(b) shows that increasing a_2 raises the concentration of cancer cells. This indicates that when the oncogenic virus reduces the death rate of cancer cells, the concentration of these cells in the body increases.

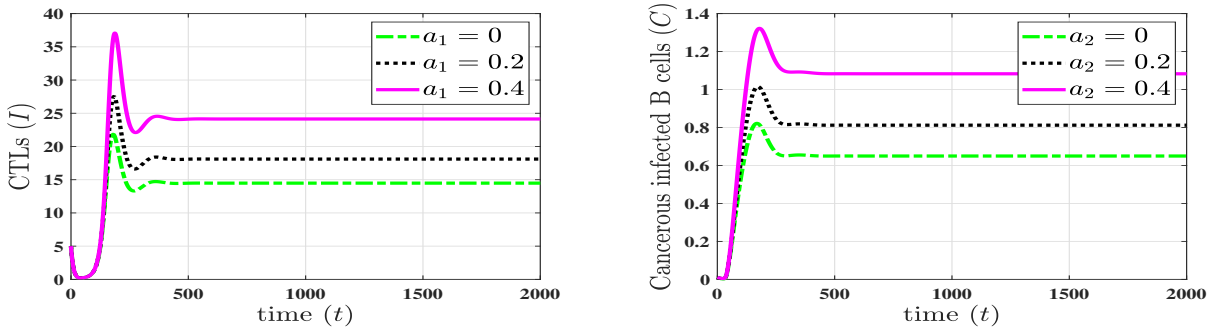

(a) **(b)**

Figure 4. (a) The impact of the oncogenic virus on CTL-mediated killing of actively infected cells (a_1). (b) The impact of the oncogenic virus on the natural death of cancerous cells (a_2).

5.2. *Effects of time delays on the model behavior*

To observe the impact of increasing the values of time delays on the system dynamics, we vary τ_1, τ_2, and τ_3 in case (ii). Figure 5 shows that increasing these delays leads to an increase in the concentration of healthy cells. In contrast, the delays decrease the concentrations of actively infected cells, latently infected cells, and cancer cells. As a result, the number of virus particles decreases. Thus, in the absence of CTLs, these delays can have a positive impact on the system.

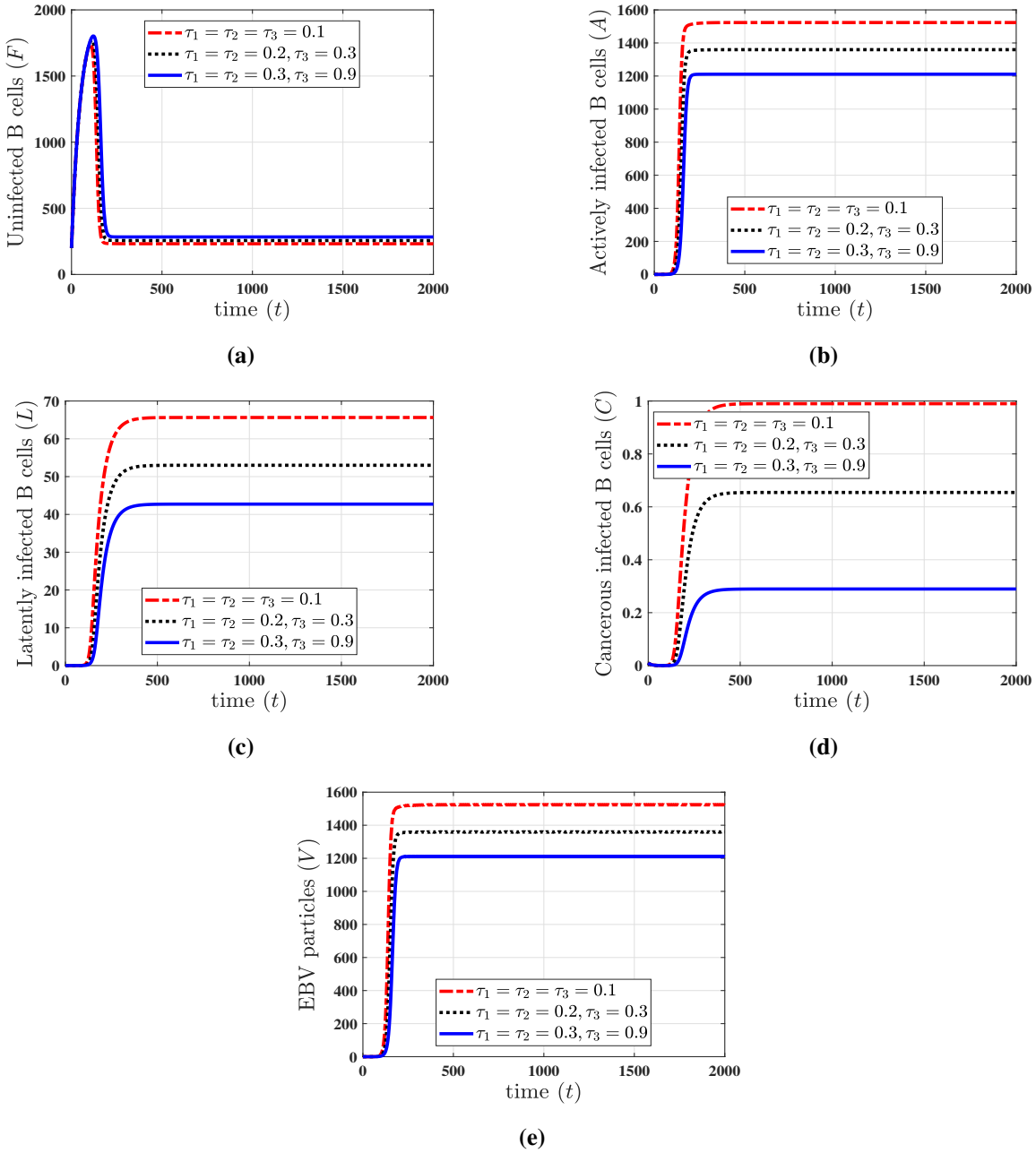

Figure 5. The impact of increasing the values of the time delays (τ_1, τ_2, and τ_3) on the dynamics of the model.

6. Sensitivity analysis

6.1. Sensitivity analysis of $\mathcal{R}_V$

To understand how different parameters affect the stability of the healthy equilibrium $\mathcal{Q}_0$, we perform a sensitivity analysis of $\mathcal{R}_V$. The analysis identifies how $\mathcal{R}_V$ is affected by variations in the parameters. The normalized forward sensitivity index of $\mathcal{R}_V$ w.r.t a parameter p is defined by [37]

$$\Pi_p^{\mathcal{R}_V} = \frac{\partial \mathcal{R}_V}{\partial p} \cdot \frac{p}{\mathcal{R}_V},$$

where $\mathcal{R}_V$ is a differentiable function of p. Using the values listed in Table 1 with $\alpha = 10^{-7}$ and $\rho_1 = 10^{-5}$, we compute the sensitivity indices of $\mathcal{R}_V$ as given in Table 2 and visualized in Figure 6(a). From these results, we observe the following:

(i) The production rate of uninfected cells (θ), the infection rate (ρ_1), and the proliferation rate of EBV (η) are the parameters that increase $\mathcal{R}_V$ when their values increase;

(ii) The conversion rate of actively infected cells into latent cells (ρ_2), the death rate of active cells (ϵ_2), the death rate of uninfected cells (ϵ_1), the decay rate of EBV (ϵ_5), and the delay parameters r_1 and τ_1 are the parameters that reduce $\mathcal{R}_V$ when their values increase;

(iii) Increasing (or reducing) any of the parameters η, θ, ρ_1, ϵ_1, or ϵ_5 by 10% increases (or reduces) $\mathcal{R}_V$ by 10%;

(iv) Increasing ρ_2 by 10% reduces $\mathcal{R}_V$ by 0.476%;

(v) Increasing ϵ_2 by 10% decreases $\mathcal{R}_V$ by 9.524%;

(vi) Increasing r_1 or τ_1 by 10% reduces $\mathcal{R}_V$ by 1%.

Based on these results, the parameters η, θ, and ρ_1 contribute to the initiation of an EBV infection, whereas ρ_2, ϵ_1, ϵ_2, ϵ_5, r_1, and τ_1 play important roles in maintaining the stability of the healthy state and preventing the initiation of an EBV infection. In addition, the parameters η, θ, ρ_1, ϵ_1, ϵ_2, and ϵ_5 are identified as the most sensitive parameters affecting $\mathcal{R}_V$.

Table 2. Sensitivity indices of $\mathcal{R}_V$.

Parameter P	η	θ	ρ_1	ρ_2	ϵ_1	ϵ_2	ϵ_5	r_1	τ_1
$\Pi_p^{\mathcal{R}_V}$	1	1	1	-0.0476	-1	-0.9524	-1	-0.1	-0.1

6.2. Sensitivity analysis of $\mathcal{R}_I$

The normalized forward sensitivity index of $\mathcal{R}_I$ w.r.t a parameter p is defined by the following:

$$\Pi_p^{\mathcal{R}_I} = \frac{\partial \mathcal{R}_I}{\partial p} \cdot \frac{p}{\mathcal{R}_I}.$$

Using the values listed in Table 1 with $\alpha = 10^{-7}$ and $\rho_1 = 10^{-4}$, we compute the sensitivity indices of $\mathcal{R}_I$ as given in Table 3 and visualized in Figure 6(b). From these results, we note the following:

(i) The stimulation rate of CTLs (α), the production rate of uninfected cells (θ), the infection rate (ρ_1), and the proliferation rate of EBV (η) are the parameters that increase $\mathcal{R}_I$ when their values increase;

(ii) The conversion rate of actively infected cells into latent cells (ρ_2), the death rate of uninfected cells (ϵ_1), the death rate of active cells (ϵ_2), the decay rate of EBV (ϵ_5), the decay rate of CTLs (ϵ_6), and the delay parameters r_1 and τ_1 are the parameters that reduce $\mathcal{R}_I$ when their values increase;

(iii) Increasing θ by 10% increases $\mathcal{R}_I$ by 10%;

(iv) Increasing α by 10% increases $\mathcal{R}_I$ by 9.998%;

(v) Increasing η or ρ_1 by 10% increases $\mathcal{R}_I$ by 1.9996×10^{-3}%;

(vi) Increasing ρ_2 by 10% reduces $\mathcal{R}_I$ by 0.476%;

(vii) Increasing ϵ_1 or ϵ_5 by 10% reduces $\mathcal{R}_I$ by 1.9996×10^{-3}%;

(viii) Increasing ϵ_2 by 10% reduces $\mathcal{R}_I$ by 9.524%;

(ix) Increasing ϵ_6 by 10% reduces $\mathcal{R}_I$ by 9.99%;

(x) Increasing r_1 or τ_1 by 10% reduces $\mathcal{R}_I$ by 1%.

Based on these results, the parameters α, η, θ, and ρ_1 contribute to the activation of the CTL immune response against an EBV infection. In contrast, the parameters ρ_2, ϵ_1, ϵ_2, ϵ_5, ϵ_6, r_1, and τ_1 contribute to the inhibition of CTL immunity. Moreover, the parameters α, θ, ϵ_2, and ϵ_6 are identified as the most sensitive parameters affecting $\mathcal{R}_I$.

Table 3. Sensitivity indices of $\mathcal{R}_I$.

Parameter P	α	η	θ	ρ_1	ρ_2	ϵ_1	ϵ_2	ϵ_5	ϵ_6	r_1	τ_1
$\Pi_p^{\mathcal{R}_I}$	0.9998	1.9996×10^{-4}	1	1.9996×10^{-4}	-0.0476	-1.9996×10^{-4}	-0.9524	-1.9996×10^{-4}	-0.999	-0.1	-0.1

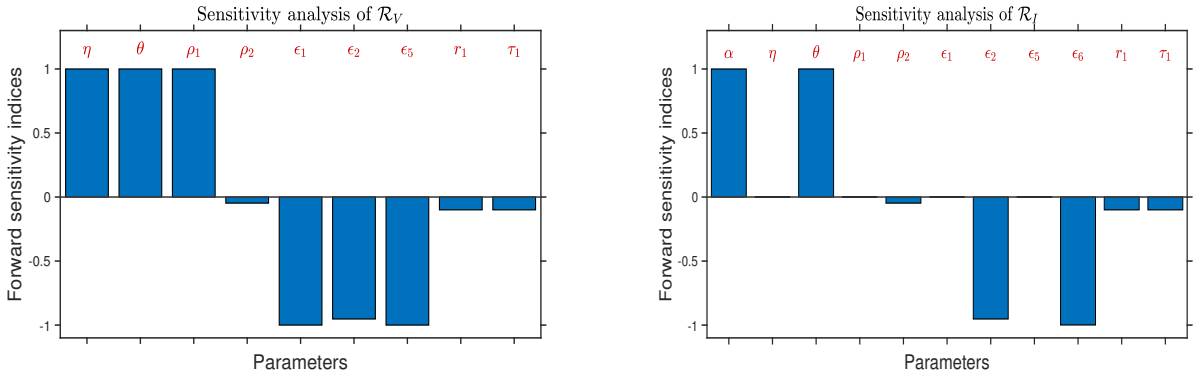

(a) **(b)**

Figure 6. (a) The normalized forward sensitivity indices of $\mathcal{R}_V$. (b) The normalized forward sensitivity indices of $\mathcal{R}_I$.

7. Discussion and conclusions

A strong link has been found between EBV infections and many cancers [4]. Thus far, no effective treatments for latent EBV infections have been identified [1]. This has emphasized the urgent need to understand the pathogenesis of EBV infections and its relation to cancer. Mathematical models can help the ongoing clinical trials in developing effective therapies for EBV infection. This paper proposed a delayed EBV model. The model has three equilibrium points as follows:

(1) The healthy equilibrium Q_0, which is stable if $\mathcal{R}_V < 1$. This point reflects the case of a person with no EBV infection.

(2) The EBV immune-inactive equilibrium Q_1, which is stable if $\mathcal{R}_V > 1$ and $\mathcal{R}_I < 1$. This equilibrium represents an individual with an EBV infection and an inactive CTL immune response.

(3) The EBV immune-active equilibrium Q_2, which is stable if $\mathcal{R}_I > 1$. This equilibrium represents an individual with an EBV infection and an active CTL immune response.

The numerical simulations confirmed the stability results of Theorems 4.1–4.3. Since the numerical simulations demonstrate the stability of the equilibria for three different sets of initial conditions, this suggests their potential global stability, which may be rigorously established in future work. Furthermore, we found that increasing the value of a_1, which measures the role of EBV in weakening the ability of CTLs to kill infected cells, increases the concentration of infected B cells in the body. Consequently, the number of recruited CTLs will be higher. This result suggests that immune escape should not be interpreted as a reduction in the number of CTLs, but rather as a reduction in their functional ability to eliminate infected cells. Although larger values of a_1 increase the total density of CTLs, their ability to eliminate infected cells is diminished. Moreover, increasing the value of a_2, which measures the role of the EBV in impairing the natural death of cancer cells, increases the concentration of cancer cells in the body. In addition, we observed that increasing the values of the time delays in the absence of CTLs in model (2.1) raises the concentration of healthy cells and reduces the concentrations of infected cells and cancer cells. From a biological perspective, this suggests that therapeutic interventions capable of slowing the establishment of active infection, the transition to latency, or the progression to cancer may have beneficial effects similar to those predicted by larger delay values in the model. Although no therapy is specifically designed to increase time delays, several antiviral and anticancer therapies may indirectly produce analogous effects by slowing the underlying biological mechanisms represented by these delays. Additionally, the results show that $\mathcal{R}_V$ is most sensitive to the parameters η, θ, ρ_1, ϵ_1, ϵ_2, and ϵ_5. On the other hand, $\mathcal{R}_I$ is most sensitive to the parameters α, θ, ϵ_2, and ϵ_6. Therefore, these parameters should be carefully estimated, as they play crucial roles in the establishment of an EBV infection and the activation of CTL immunity. Notably, the production rate of uninfected cells (θ) and the death rate of actively infected cells (ϵ_2) exert equal effects on $\mathcal{R}_V$ and $\mathcal{R}_I$. In addition, the viral proliferation rate (η), the infection rate (ρ_1), the death rate of uninfected cells (ϵ_1), and the decay rate of EBV (ϵ_5), which strongly affect $\mathcal{R}_V$, have negligible effects on $\mathcal{R}_I$. This suggests that once EBV infection is established, the persistence of CTL immunity predominantly depends on the activation and survival of immune cells rather than on viral replication itself. Overall, the sensitivity analyses indicate that $\mathcal{R}_V$ is primarily governed by viral replication and infection processes, whereas $\mathcal{R}_I$ is mainly regulated by immune activation and CTL dynamics. It

should be noted that although the sensitivity analyses indicate that the basic reproduction number $\mathcal{R}_V$ increases with the production rate of uninfected B cells (θ), this does not imply that reducing θ is a desirable therapeutic intervention. In fact, lowering θ could impair the host immune system and have detrimental clinical consequences. The positive sensitivity index simply indicates that a larger pool of susceptible target cells can facilitate viral infection. In contrast, parameters directly associated with viral infection and replication, such as the infection rate (ρ_1) and the proliferation rate (η), represent more plausible therapeutic targets because reducing these parameters may suppress the EBV infection without affecting the production of immune cells. Compared with existing works, the model suggested in this paper is the first model that studies the oncogenic effect of the EBV with a mathematical analysis. The present study faces both mathematical and biological challenges. Mathematically, proving the local stability of Q_1 and Q_2 for positive delays requires advanced analytical techniques, including imaginary-root analyses and the Hopf bifurcation theory. Biologically, the scarcity of experimental data necessitated the use of some assumed parameter values. One limitation of the present model is that it assumes a unidirectional progression from active infection to latency. In reality, the EBV can switch between latent and lytic phases under certain biological conditions [38]. A further limitation is that the local stability of Q_1 and Q_2 was only established for zero time delays. Another important limitation is that some parameter values were obtained from published studies, whereas others were assumed. When empirical data become available, the results can be tested and the model can be used to do the following:

(i) Determine the parameter values that shift the system from a healthy state (Q_0 stable) to an EBV-infected cancer state with inactive CTL immunity (Q_1 stable), and further to an EBV-infected cancer state with active CTLs (Q_2 stable);

(ii) Test the impact of the oncogenic virus on the natural death of cancer cells and the killing rate of CTLs;

(iii) Examine the impact of time delays on the system dynamics;

(iv) Develop therapies that mimic the effects of the time delays.

Model (2.1) can be extended by the following:

(i) Establishing the local stability of Q_1 and Q_2 for positive time delays;

(ii) Proving the global stability of the equilibrium points by constructing suitable Lyapunov-Krasovskii functionals that incorporate the delay terms and establishing the stability under appropriate threshold conditions;

(iii) Considering the delays that can occur during the viral replication or immune response stimulation;

(iv) Incorporating the spatial distribution of the model components;

(v) Using fractional derivatives to test the memory effect on the model behavior;

(vi) Incorporating a multistage progression process, distributed delays, or stochastic mechanisms to represent the long-term progression from latent EBV infection to cancer;

(vii) Investigating the possibility of delay-induced Hopf bifurcations and periodic solutions that can arise from variations in the delay parameters;

(viii) Incorporating a reactivation pathway from latent cells to actively infected cells.

Author contributions

Azizah Alrajhi: Supervision, validation, conceptualization, writing-review and editing; Afnan Al Agha: Methodology, investigation, formal analysis, writing-original draft. All authors have read and approved the final version of the manuscript.

Use of Generative-AI tools declaration

The authors declare they have not used Artificial Intelligence (AI) tools in the creation of this article.

Aknowledgments

This project was funded by the Deanship of the Scientific Research (DSR) at King Abdulaziz University, Jeddah, Saudi Arabia under grant no. (IPP: 1095-247-2025). The authors, therfore, acknowledge with thanks DSR for technical and financial support.

Conflict of interest

The authors declare that they have no conflict of interest.

References

1. U. N. Mui, C. T. Haley, S. K. Tyring, Viral oncology: Molecular biology and pathogenesis, *J. Clin. Med.*, **6** (2017), 111. https://doi.org/10.3390/jcm6120111
2. K. Ahmed, S. Jha, Oncoviruses: How do they hijack their host and current treatment regimes, *Biochim. Biophys. Acta Rev. Cancer*, **1878** (2023), 188960. https://doi.org/10.1016/j.bbcan.2023.188960
3. C. L. Murall, S. Alizon, Modelling the evolution of viral oncogenesis, *Phil. Trans. R. Soc. B*, **374** (2019), 20180302. https://doi.org/10.1098/rstb.2018.0302
4. P. J. Farrell, Epstein-Barr virus and cancer, *Annu. Rev. Pathol.*, **14** (2019), 29–53. https://doi.org/10.1146/annurev-pathmechdis-012418-013023
5. L. S. Young, A. B. Rickinson, Epstein-Barr Virus: 40 Years on, *Nat Rev Cancer*, **4** (2004), 757–768. https://doi.org/10.1038/nrc1452
6. M. Kang, E. Kieff, Epstein-Barr virus latent genes, *Exp. Mol. Med.*, **47** (2015), e131. https://doi.org/10.1038/emm.2014.84
7. B. Damania, S. C. Kenney, N. Raab-Traub, Epstein-Barr virus: Biology and clinical disease, *Cell*, **185** (2022), 3652–3670. https://doi.org/10.1016/j.cell.2022.08.026
8. K. P. Michalak, W. Adamski, A system-level perspective on Epstein–Barr virus persistence: The partial lytic reactivation, *Int. J. Mol. Sci.*, **27** (2026), 3337. https://doi.org/10.3390/ijms27073337
9. S. B. Pattle, P. J. Farrell, The role of Epstein-Barr virus in cancer, *Expert Opin. Biol. Ther.*, **6** (2006), 1193–1205. https://doi.org/10.1517/14712598.6.11.1193

10. Y. Li, R. Xu, S. Mao, Global dynamics of a delayed HIV-1 infection model with CTL immune response, *Discrete Dyn. Nat. Soc.*, **2011** (2011), 673843. https://doi.org/10.1155/2011/673843
11. K. A. Pawelek, S. Liu, F. Pahlevani, L. Rong, A model of HIV-1 infection with two time delays: Mathematical analysis and comparison with patient data, *Math. Biosci.*, **235** (2012), 98–109. https://doi.org/10.1016/j.mbs.2011.11.002
12. A. M. Elaiw, A. D. Al Agha, Stability of a general HIV-1 reaction–diffusion model with multiple delays and immune response, *Phys. A*, **536** (2019), 122593. https://doi.org/10.1016/j.physa.2019.122593
13. X. Zhou, L. Zhang, T. Zheng, H. Li, Z. Teng, Global stability for a delayed HIV reactivation model with latent infection and Beddington–DeAngelis incidence, *Appl. Math. Lett.*, **117** (2021), 107047. https://doi.org/10.1016/j.aml.2021.107047
14. Y. Zhang, Z. Xu, Dynamics of a diffusive HBV model with delayed Beddington-DeAngelis response, *Nonlinear Anal. Real World Appl.*, **15** (2014), 118–139. https://doi.org/10.1016/j.nonrwa.2013.06.005
15. K. Manna, Dynamics of a delayed diffusive HBV infection model with capsids and CTL immune response, *Int. J. Appl. Comput. Math.*, **4** (2018), 116. https://doi.org/10.1007/s40819-018-0552-4
16. A. M. Elaiw, A. D. Al Agha, Global dynamics of a general diffusive HBV infection model with capsids and adaptive immune response, *Adv. Differ. Equ.*, **2019** (2019), 519. https://doi.org/10.1186/s13662-019-2448-y
17. A. R. M. Carvalho, C. M. A. Pinto, D. Baleanu, HIV/HCV coinfection model: A fractional-order perspective for the effect of the HIV viral load, *Adv. Differ. Equ.*, **2018** (2018), 2. https://doi.org/10.1186/s13662-017-1456-z
18. B. Yu, J. Shi, Z. Xue, M. Yang, X. Yang, Y. Su, Stability analysis of HCV dynamic model with saturation incidence, cellular immunity and interferon effect in intrahepatic and extrahepatic tissues, *Math. Comput. Simulation*, **216** (2024), 301–317. https://doi.org/10.1016/j.matcom.2023.09.017
19. Q. Badshah, K. S. Nisar, G. Rahman. R. P. Agarwal, S. Islam, Stochastic modeling of within host dynamics of HCV model under therapy, *Results Phys.*, **22** (2021), 103826. https://doi.org/10.1016/j.rinp.2021.103826
20. A. O. Yunus, O. A. Olanrewaju, Fractional-order modeling of vaccination strategies for measles transmission incorporating immune memory, *Virus Res.*, **367** (2026), 199718. https://doi.org/10.1016/j.virusres.2026.199718
21. A. O. Yunus, M. O. Olayiwola, Mathematical modeling of malaria epidemic dynamics with enlightenment and therapy intervention using the Laplace-Adomian decomposition method and Caputo fractional order, *Frankl. Open*, **8** (2024), 100147. https://doi.org/10.1016/j.fraope.2024.100147
22. A. O. Yunus, M. O. Olayiwola, M. O. Abanikanda, Modeling a fractional-order chlamydia dynamic with protected intimacy as a strategic control intervention, *Discov. Public Health*, **22** (2025), 491. https://doi.org/10.1186/s12982-025-00856-4
23. M. V. Krishna, Mathematical modelling on diffusion and control of COVID-19, *Infect. Dis. Model.*, **5** (2020), 588–597. https://doi.org/10.1016/j.idm.2020.08.009

24. T. Sumi, K. Harada, Immune response to SARS-CoV-2 in severe disease and long COVID-19, *iScience*, **25** (2022), 104723. https://doi.org/10.1016/j.isci.2022.104723
25. A. M. Elaiw, A. D. Al Agha, S. A. Azoz, E. Ramadan, Global analysis of within-host SARS-CoV-2/HIV coinfection model with latency, *Eur. Phys. J. Plus*, **137** (2022), 174. https://doi.org/10.1140/epjp/s13360-022-02387-2
26. C. Li, J. Xu, J. Liu, Y. Zhou, The within-host viral kinetics of SARS-CoV-2, *Math. Biosci. Eng.*, **17** (2020), 2853–2861. https://doi.org/10.3934/mbe.2020159
27. A. O. Yunus, M. O. Olayiwola, A mathematical model for assessing vaccination's efficacy as a preventative strategy against newly emerging COVID-19 variants, *Vacunas*, **26** (2025), 500392. https://doi.org/10.1016/j.vacun.2025.500392
28. A. Elsonbaty, T. M. Al-shami, A. El-Mesady, Unveiling the dynamics of meningitis infections: A comprehensive study of a novel fractional-order model with optimal control strategies, *Bound. Value Probl.*, **2025** (2025), 48. https://doi.org/10.1186/s13661-025-02034-6
29. A. El-Mesady, A. Aldakhil, A. Elsonbaty, On nonlinear dynamical analysis of a fractional-order two-strains Nipah virus model, *Partial Differ. Equ. Appl. Math.*, **11** (2024), 100900. https://doi.org/10.1016/j.padiff.2024.100900
30. H. M. Ali, A. M. S. Mahdy, A. El-Mesady, Investigation of stability criteria and optimal control measures for a fractional-order model of human papillomavirus infection and cervical cancer, *Int. J. Biomath.*, 2025. https://doi.org/10.1142/S1793524525500639
31. J. Zhao, J. P. Tian, Spatial model for oncolytic virotherapy with lytic cycle delay, *Bull. Math. Biol.*, **81** (2019), 2396–2427. https://doi.org/10.1007/s11538-019-00611-2
32. Z. Wang, Z. Guo, H. Peng, A mathematical model verifying potent oncolytic efficacy of M1 virus, *Math.l Biosci.*, **276** (2016), 19–27. https://doi.org/10.1016/j.mbs.2016.03.001
33. A. Al Agha, H. Al Garalleh, Oncolysis by SARS-CoV-2: Modeling and analysis, *AIMS Mathematics*, **9** (2024), 7212–7252. https://doi.org/10.3934/math.2024351
34. J. K. Hale, S. M. V. Lunel, *Introduction to functional differential equations*, New York: Springer, 1993. https://doi.org/10.1007/978-1-4612-4342-7
35. Y. Kuang, *Delay differential equations: With applications in population dynamics*, Cambridge: Academic Press, 2012.
36. F. A. Rubio, H. M. Yang, A mathematical model to evaluate the role of memory B and T cells in heterologous secondary dengue infection, *J. Theor. Biol.*, **534** (2022), 110961. https://doi.org/10.1016/j.jtbi.2021.110961
37. N. Chitnis, J. M. Hyman, J. M. Cushing, Determining important parameters in the spread of malaria through the sensitivity analysis of a mathematical model, *Bull. Math. Biol.*, **70** (2008), 1272–1296. https://doi.org/10.1007/s11538-008-9299-0
38. T. Murata, T. Tsurumi, Switching of EBV cycles between latent and lytic states, *Rev. Med. Virol.*, **24** (2014), 142–153. https://doi.org/10.1002/rmv.1780